



Commission 2

Menthon-Saint-Bernard DAYS – 24st –26th May, 2011

Paper 2-16

Corrosion of buried pipelines detected on ER-probes Comparison with MFL ILI results

Dr. Nick Kioupis,
Hellenic Gas Transmission System Operator (DESFA) S.A.
n.kioupis@desfa.gr

Abstract

Corrosion rate recordings on Electrical Resistance (ER) probes, connected to natural gas transmission pipelines of DESFA, are interpreted. Based on these results, various AC corrosion behaviours as well as telluric currents corrosion are discovered. The corrosion phenomena are very sensitive to the local electrical conditions and soil environment. Correlations between spread resistance, AC current density, AC voltage and corrosion rate are examined for every corrosion case. Eventually, the corrosion rates taken from the recordings on ER probes are compared with In-Line Inspection (ILI) results of metal losses given by means of intelligent pigging technique with the Magnetic Flux Leakage (MFL) method. Interpretations of the differences observed between the results of corrosion rates of ER-probes and ILI data are discussed. Various factors give rise to several measurement uncertainties which render questionable the AC corrosion rate estimated from MFL ILI data.

Abbreviations

CP : Cathodic Protection

ER : Electrical Resistance

MFL : Magnetic Flux Leakage

ILI : In Line Inspection

ATA : Anti-parallel Thyristors Arresters

AVACF : Alternating Voltage Arresters of Continuous Function

OCP : Open Circuit Potential

AC : Alternating Current

DC : Direct Current

Keywords

pipelines, cathodic protection, AC corrosion, telluric currents, ER probes, spread resistance, intelligent pigging, metal loss.

Introduction

As the well coated pipelines may be more vulnerable to AC/DC stray currents and telluric disturbance [1-3], the recordings of time-stamped corrosion rates and the close monitoring of CP operation, become more important for the efficient management of corrosion protection. In this context, the ER probes with data logging and quick presentation of time-stamped results are an effective means for the evaluation of the stray currents impact on pipeline corrosion.

This study focused on the field test results taken by an investigation of AC corrosion in the natural gas main transmission pipeline of Greece. Corrosion rates and various quantities of CP function and AC/DC interference were recorded at ER probes installed near the pipeline.

Corrosion rates estimated from ER probes recordings were compared with corrosion rates assessed by metal loss data taken from MFL ILI (intelligent pigging) reports. Literature review and investigation of several scenarios were given to explain the deviations between the two methods, emphasizing at the ability of MFL ILI technique for accurate evaluation of AC corrosion rate.

Experimental Procedure

The use of ER probes is particularly useful for assessing the risk of AC corrosion or corrosion by DC or quasi-DC stray currents on buried pipelines. More details about ER method and related equipment for the recording of corrosion rate and CP effectiveness have been reported in the literature [4-6]. To confirm the CP effectiveness of a buried pipeline, an ER probe is electrically connected to the pipeline and placed in the soil at a depth close to the burial of the pipeline. The probe acts as an artificial defect in the insulating coating and the rate of corrosion is used to assess the risk of pipeline corrosion when exposed through a defect in the insulating coating of the similar chemical and electrical environment in which the probe is located (Fig.1).

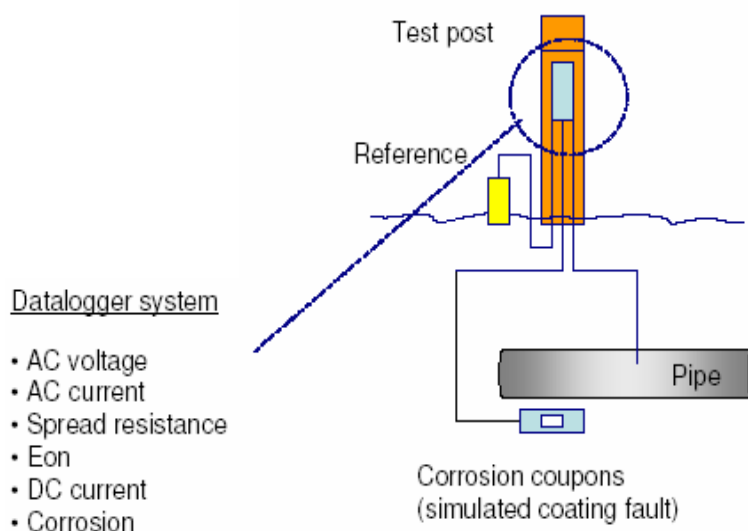


Fig. 1. Schematic of the data logger system with ER probe.

The method of ER measurement was applied as an alternative measurement of corrosion rates instead of the conventional methods for determining the weight loss of corrosion coupons. The main disadvantage of measuring weight loss was that the coupon should be removed from the environment in which it is exposed, transported to the laboratory for cleaning and weighing, procedures which are impractical and time consuming. In contrast, the ER method allows a continuous recording and requires no additional excavation to assess corrosion of the probe. It provides the corrosion rate through the loss of thickness of the exposed ER probe, a parameter which essentially completes the traditional electrical CP measurements.

However, the lifetime of the measurement is identical to the lifetime of the ER probe, where in an environment undergoing rapid corrosion, especially in thin probes, it is relatively short (order of magnitude $\frac{1}{2}$ - 6 months). Thick probes have disadvantage in accuracy and sensitivity of the measurement of rapid corrosion rates. This is the main reason that thin probes are suggested for more accurate recording of slow corrosion rates whereas thicker corrosion probes fit better for longer recording time or in case of fast corrosion rates. Additionally, the data logging system generally required an effective protection from transient overvoltages and overcurrents, otherwise the recording was prone to untimely disruptions.

Two types of ER probes data logger were used, i.e. type 1 and type 2. Some parameters recorded by the type 1 data logger were corrosion rate (V_{corr}), AC voltage (U_{ac}), AC current density (i_{ac}), calculated thickness (d), spread resistance (R_s). The type 1 data logging system did not record DC quantities (only DC potentials were occasionally recorded by a different voltage recording system). The type 2 data logging system, additionally recorded DC current density, (i_{dc}) and DC potential on, (E_{on}). In addition, the DC potential off (E_{off}) was calculated by the subtraction from E_{on} of the IR drop meant for the product of DC current with spread resistance.

General experimental conditions

At three different positions of the cathodically protected NG main transmission pipeline of Greece (Fig.2), ER probes were installed. Four distinct types of corrosion behavior were found, which are detailed in Table and analyzed further below (see case studies no. 1,2,3,4). The ER probes were buried at a depth of about 1 meter, in pairs and in adjacent positions, spaced about 1 meter between them. The pipeline, coated with 3 layer PE with heat shrinkable sleeves at girth welds and polyurethane tar coating of the buried valves, was well isolated from foreign structures, protected with average total DC current densities less than $1\mu A/m^2$. The depth of cover of the natural gas pipeline at this point was about 1,5m. CP was provided with one rectifier per section, isolated through buried monolithic insulating joints. Every data logging system (system 1 or 2) was recording with an hourly frequency the corrosion rates as well as the characteristic electrical and CP parameters, as detailed above.

The exposed metal surface of every ER probe was $0,4cm^2$ and the total exposed metal area per installation site was $0,8cm^2$. Three electrically separate CP areas of the pipeline with the respective case studies, shown on Fig. 2 and Table 1, were involved, as follows.

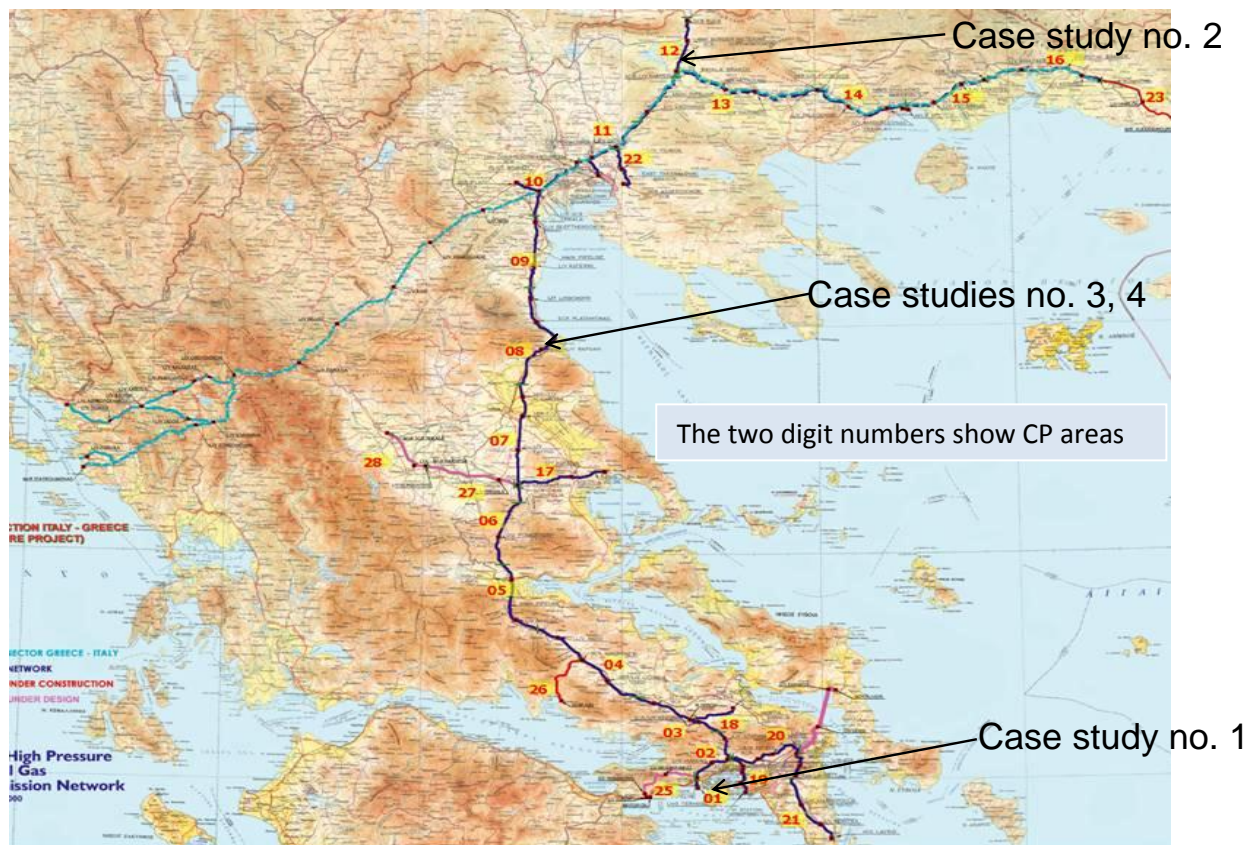


Fig. 2. Map of the Greek Natural Gas Transmission System indicating the positions of the ER probes with the corresponding corrosion case studies.

- CP area 2 (2,3-47,3 km)-Case study no.1: A couple of ER probes (tag no. 110 and no.124) of nominal thickness 100 μ m were monitored. The ER probes were mounted near the southern end of the pipeline at chainage 2.5 km at a crossing with a foreign cathodically protected fuel pipeline. The pipeline was subject to AC influence caused by AC high voltage overhead powerlines in the vicinity. In this region, the AC voltage had been already reduced by the operation of Alternating Voltage Arresters of Continuous Function (AVACF), i.e. special electronic devices with capacitive performance [7]. CP was provided by one rectifier located at 40,1km. The rectifier during the measurement was operating in potentiostatic mode, at -1,45V. The total current typically ranged between 40 and 70mA giving an average current density of 0,5 μ A/m². Interference from CP systems of foreign lines was considered hardly significant, due to insulation measures taken at crossings with the foreign pipelines. The ER probes were buried in a corrosive swampy soil with high ground water table. The soil had high content of CaCO₃ while medium in clay. As it was at a close distance (300-400m) from the sea, the ground water is believed to be rich in chlorides. The soil pH was slightly alkaline (pH 8.2). The soil resistivity had been measured less than 1 Ω -m.
- CP area 12 (478,6-512km) – Case study no. 2: A couple of ER probes were monitored (tag no.196 and no.244) of nominal thickness 500 μ m and 100 μ m respectively. The ER probes were installed at chainage 483,3 km. The pipeline was subject to strong AC influence caused by AC high voltage overhead powerlines in the vicinity. In this CP area, only DC-decoupling devices, a kind of Anti-parallel Thyristor Arresters (ATA) activating at 25Vrms, were operating [7,8]. CP was provided by one rectifier located at 482,2km. During the recordings, the

rectifier operated in potentiostatic mode at -1,30V. The average total DC current was around 80 mA, corresponding to a DC current density of $0.83\mu\text{A}/\text{m}^2$. The soil where the ER probes were buried was very conductive. By the low spread resistance ($0,006\ \Omega\text{m}^2$) and the AC voltage, the soil resistivity was estimated in the order of $1\Omega\text{-m}$.

- CP areas 4-9 (83,3-377,0km)-Case studies no. 3 and no. 4: A couple of ER probes (tag no. 35 and 36) with nominal thickness of $100\mu\text{m}$ were monitored. ER probes were installed at 304,4 km. The results refer to two different time periods of recordings, namely case studies no. 3 and no. 4. This long pipeline section extending from 83,3 to 377km, was interfered by AC high voltage overhead powerlines and by telluric currents. During the monitoring, the AC mitigation system was not in operation. There were originally six electrically independent CP areas, but during the measurements, CP areas behaved collectively as an electrically unified pipeline section due to the bridged intermediate insulating joints. CP was provided by one rectifier located at 198,3 km. The rectifier was galvanostatically operating, providing DC current around 100mA, corresponding to a DC current density of $0.14\ \mu\text{A}/\text{m}^2$. From the average value of spread resistance and AC voltage, the soil resistivity was estimated in the order of $10\ \Omega\text{-m}$.

Table 1 Examined case studies of ER probes corrosion
(AC: effect of induced AC currents, T: effect of telluric currents)

Case no.	Probe ID	Area (cm ²)	Thickness (mm)	Pipeline location	CP area	Influence type	AC mitigation	Recording period	important corrosion (yes/no)	Main cause of corrosion	Recorder type
1	110	0.4	100	2.5	2	AC	capacitive, continuous function overvoltage arresters	phases 1,2,3 (Nov.2005-Jan.2006)	YES	AC	1
	124	0.4	100								
2	196	0.4	500	483.3	12	AC	anti-parallel thyristors activated at 25Vrms	July-Aug. 2006	YES	AC	2
	244	0.4	100								
3	35	0.4	100	304.4	4-9	T + AC	NO	one month after initial recording (june-july 2006)	YES (during CP fault)	AC	1
	36	0.4	100								
4	35	0.4	100	304.4	4-9	T + AC	NO	during initial recording (june 2006)	NO	T	1
	36	0.4	100								

Results and Discussion

Case study no. 1, characterized by AC corrosion at low AC voltage

ER probes of case study no. 1 were sometimes disconnected and reconnected to the cathodically protected natural gas pipeline. Therefore, the ER probes were alternately subjected to either the effect of the combination of CP and AC voltage as long as being connected to the pipeline or the effect of natural corrosion at OCP (marked as NC) as long as disconnected from the pipeline. During NC times, no significant corrosion was detected.

During some periods, the corrosion rate was recorded in real time. In periods of no recording, an average corrosion rate was derived solely from metal thicknesses (derived by the ER measurement), at the end of the previous and at the beginning of next recording time.

The bar chart in Fig. 3 indicates the progressive development of ER probes corrosion rates. At least three distinct temporal phases of corrosion were evident.

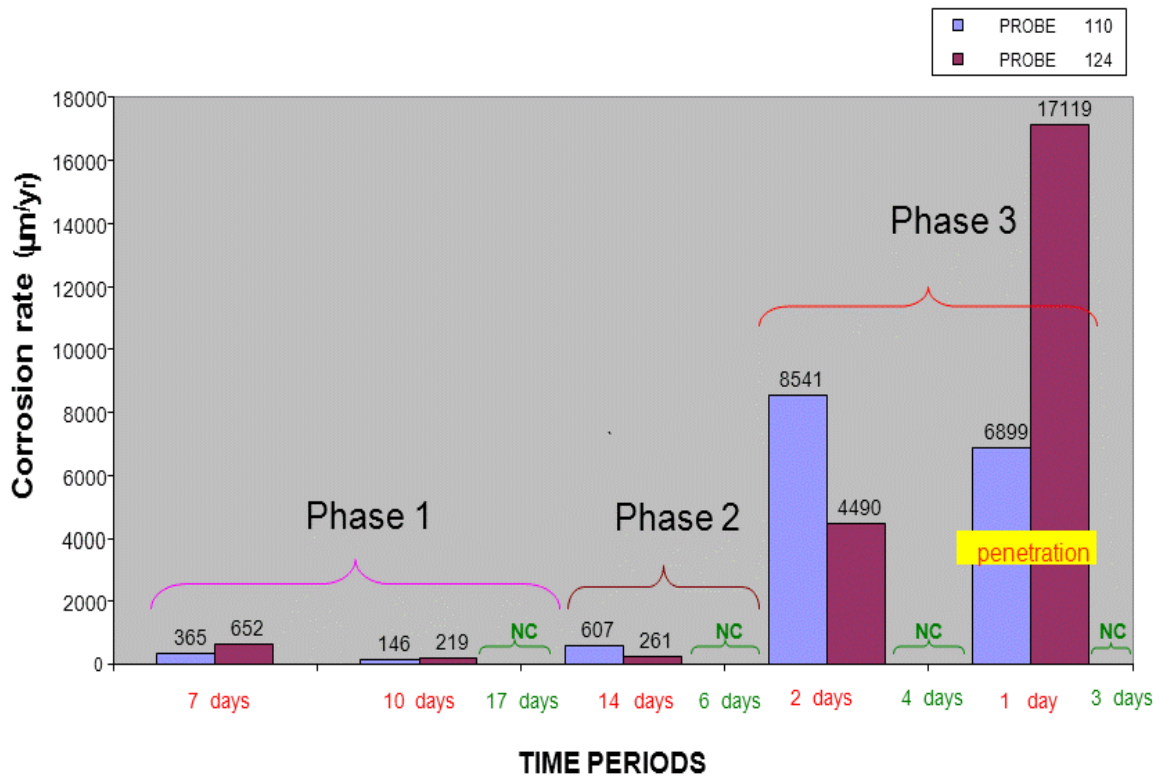


Fig. 3. Corrosion rates of case study no. 1. (NC: Natural Corrosion at OCP periods)

Results of phase 1

The corrosion had an initially high velocity with lack of incubation period. However, after the first week, the corrosion slowed down, which could be attributed to a decrease in the average level of AC voltage (Fig.3).

Results of phase 2

The corrosion products formed during the initial corrosion period gave rise to a prolongation of the time until onset of AC corrosion (i.e. incubation time). The corrosion process was characterized by sharp peaks of instantaneous corrosion rates, as illustrated by the average of 16 measurements plot. These instantaneous corrosion rates coincided with the peaks of AC voltage and respective AC current density (Fig.4).

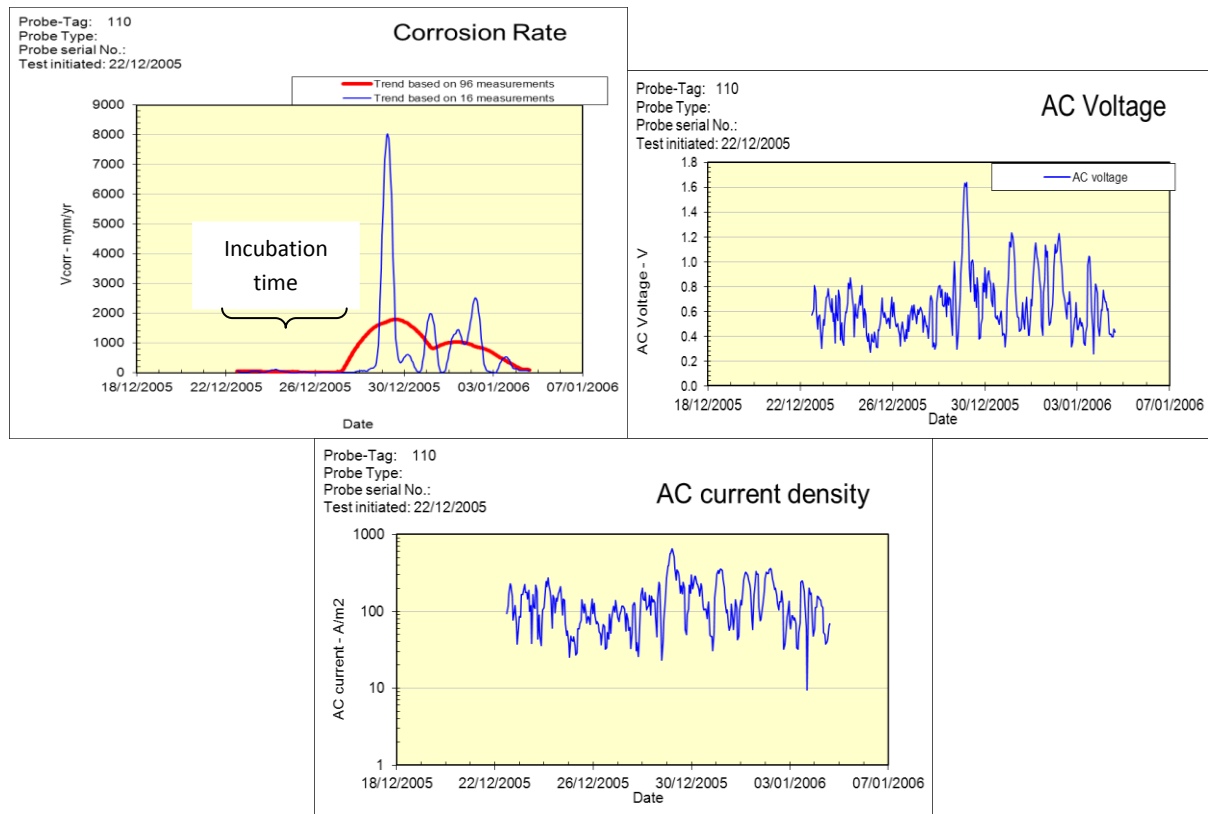


Fig. 4. Corrosion rate and respective AC voltage and AC current density vs. time during phase 2 of case study no. 1.

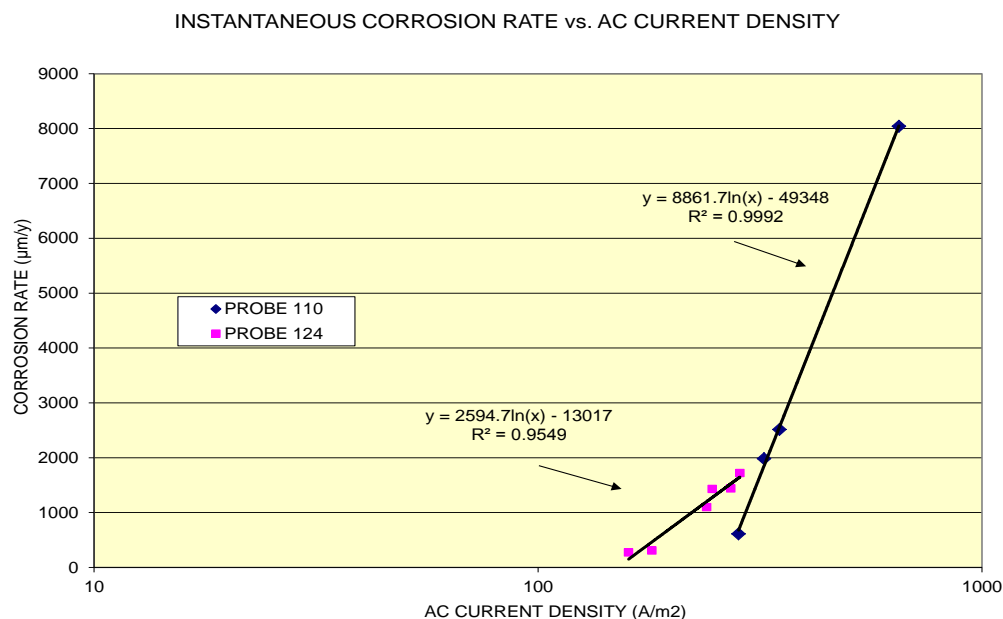


Fig. 5 Correlation of instantaneous corrosion rate with AC current density (phase 2 of case study no.1).

Essentially, the instantaneous corrosion rates followed a linear relationship with the logarithm of the respective instantaneous AC current densities (Fig. 5).

In this case, the AC corrosion criterion for AC current density was estimated at 100A/m² leading to a safe level for AC voltage only 0,5-0,6V, nearly ten times lower than the 4V limit, considered safe according to one of the criteria established from specifications [9], showing that the risk assessment of AC corrosion likelihood should

not be based solely on the criterion of AC voltage, as also dictated by the same specification.

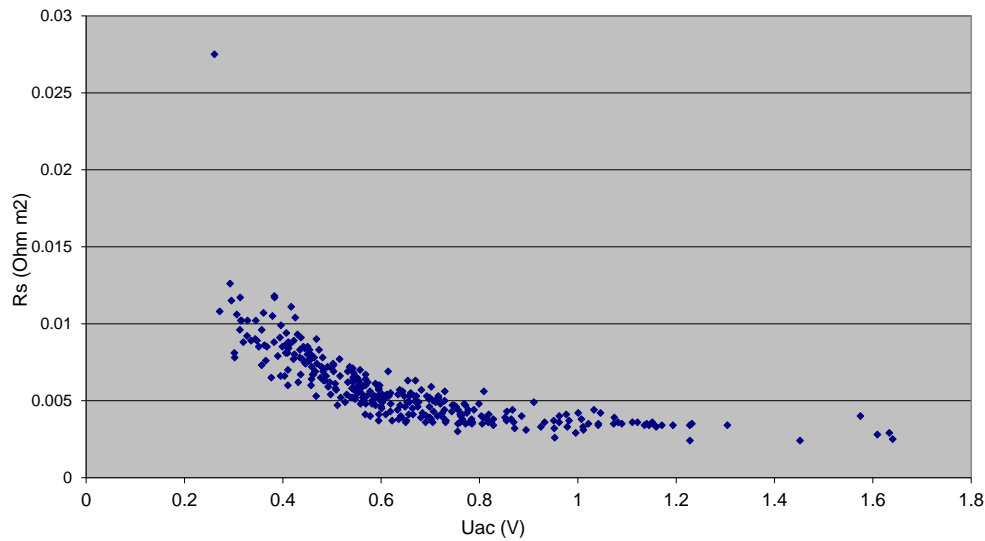


Fig. 6. Fluctuation of spread resistance with AC voltage-case study no.1.

The process of AC corrosion in case study no.1 was characterized by low spread resistance being reduced at any increase of AC voltage and vice versa, a phenomenon depicted in Fig.6. Therefore, any slight increase in AC voltage above 0,5V to 1V range led to a sharp increase in the AC current density culminating in AC corrosion [10]. At the higher values of induced AC voltage, the spread resistance tended towards a low limit; this limit was insensitive to any further increase of AC voltage. This could be explained by the alkalization mechanism of AC corrosion and the depolarizing AC effect, whereby the elevation of the AC voltage could increase the local pH and the DC current density at the metal/soil interface, catalyzing the iron dissolution [11].

Results of phase 3

As shown in Fig. 3, after a certain time, the rate of corrosion was rapidly accelerated. This observation contradicted previous reports of reduction of AC corrosion rate with time [1]. During this final period, both ER probes with remaining metal thickness of 46.9 μm and 18.9 μm respectively, were perforated by AC corrosion during one day of exposure. During this short time, the corrosion rate reached extremes, higher than 17 mm/yr. One possible explanation for this behavior was a sudden 150mV shift of the DC potential towards negative direction. Although such an extreme acceleration of corrosion was initially surprising, it has been demonstrated that the AC corrosion rate can theoretically reach extremes up to 100mm/yr [12]. Furthermore, a synergistic effect of higher induced AC voltage and a moderate excess of cathodic polarization can also accelerate AC corrosion [9].

Case study no.2, characterized by severe AC corrosion at high AC voltage

Case study no. 2 comprised a form of AC corrosion occurring in conductive soils at high AC voltage levels (above 10 V) along with frequent activation and deactivation of ATA devices. As far as AC corrosion is concerned, an effective reduction of the AC voltage was not achieved. AC voltage was varying within the range 10 to 30V with remarkably high AC current densities, multiples of 1000A/m^2 (Fig. 7). Evidently, the ATA were not able to reduce the AC voltage to a level lower than 10V, so the criterion of the AC voltage was not met [9]. Additionally, the spread resistance was almost constant and independent of the AC voltage.

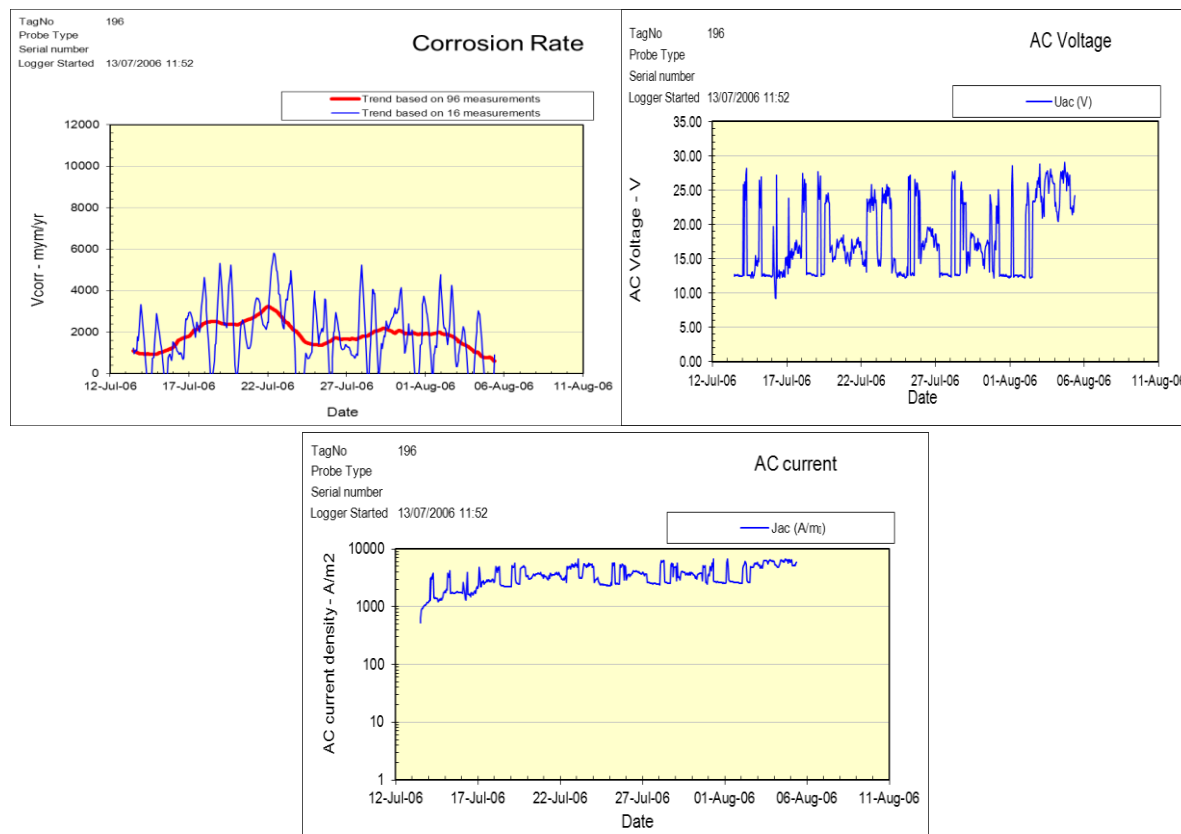


Fig. 7. Corrosion rate, AC voltage and AC current density vs. time of case study no.2.

In Fig. 7, it can be observed that there were plateaus of the lower levels of AC voltage and AC current density. These occurred during periods of activated ATA. Simultaneously an anodic shift of DC potential and DC current density was evident. The inverse happened as long as the ATA were inactive, i.e. DC potential and DC current density tended towards cathodic values during higher levels of AC voltage (Fig. 8). These results confirmed the findings reported in previous works [7,8].

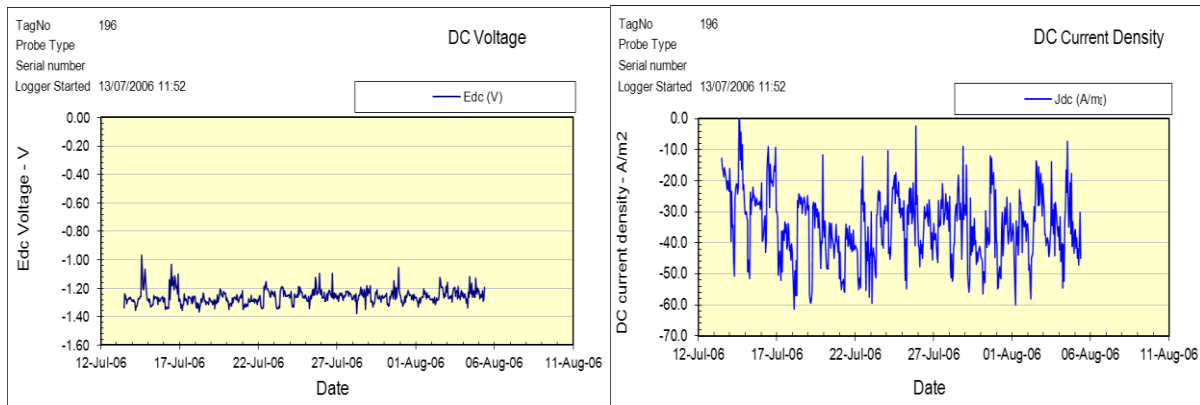


Fig. 8. DC potential on and DC current density vs. time of case study no.2.

As expected, the peaks of the instantaneous corrosion rates correlated directly with the peaks of the AC voltage and AC current density, especially when the probe remained for a longer time at high AC voltage. However, high instantaneous corrosion rates were also obtained during the low level plateaus of the AC voltage (in the range 12-16 V), especially after a prolonged stay on every of these plateaus. Eventually, the average corrosion rates generally followed the trend of the average AC voltage levels.

The above observations suggested that the relationship of AC corrosion with AC parameters was not direct. This could be interpreted by two counterbalancing phenomena associated with the synergistic effects of DC parameters on AC corrosion. These phenomena are described below.

On the one hand, lower values of AC voltage were accompanied by more anodic DC potentials and currents due to activated ATA which contributed to the acceleration of corrosion probably due to AC corrosion intensified by anodic DC potential shift as case study no. 3 suggests (see below), and/or by the formation of galvanic cells between pipeline and earthing electrodes through the DC conductive ATA.

On the other hand, during higher values of AC voltage (i.e. during inactive ATA periods), as normally expected, AC corrosion was also on the rise, this time as a result of higher AC and more cathodic DC current densities. Of particular interest is that the DC current density was unusually high (reaching levels up to 60 A/m²). The DC current was fluctuating in proportion to the AC current, suggesting the AC current was rectified probably as a result of faradaic rectification [13] which has been theoretically proved [14] as well.

Case study no. 3, characterized by AC corrosion associated with CP interruption/fault

This AC corrosion type was triggered by a CP interruption or fault. (Fig. 9). During the period of normal CP, no corrosion was detected despite the relatively negative CP level (median on-potential -1,34 V with slow negative deviations up to -1,89 V). Specifically, as the rectifier was operating in galvanostatic mode, for an unknown reason, maybe an accidental contact of the pipe with a foreign grounded structure, the CP potential dropped to anodic levels, around -0,74V, for a two weeks period. After that it became back to normal. During the time of CP fault, the corrosion rates increased dramatically whereas the instantaneous corrosion rates were fluctuating in

accordance to the AC voltage fluctuations during the same period. The escalation of the instantaneous corrosion rate at every AC voltage peak, suggested that this corrosion process was likely related to the AC interference. The AC current density was roughly constant and below the threshold of 100 A/m^2 .

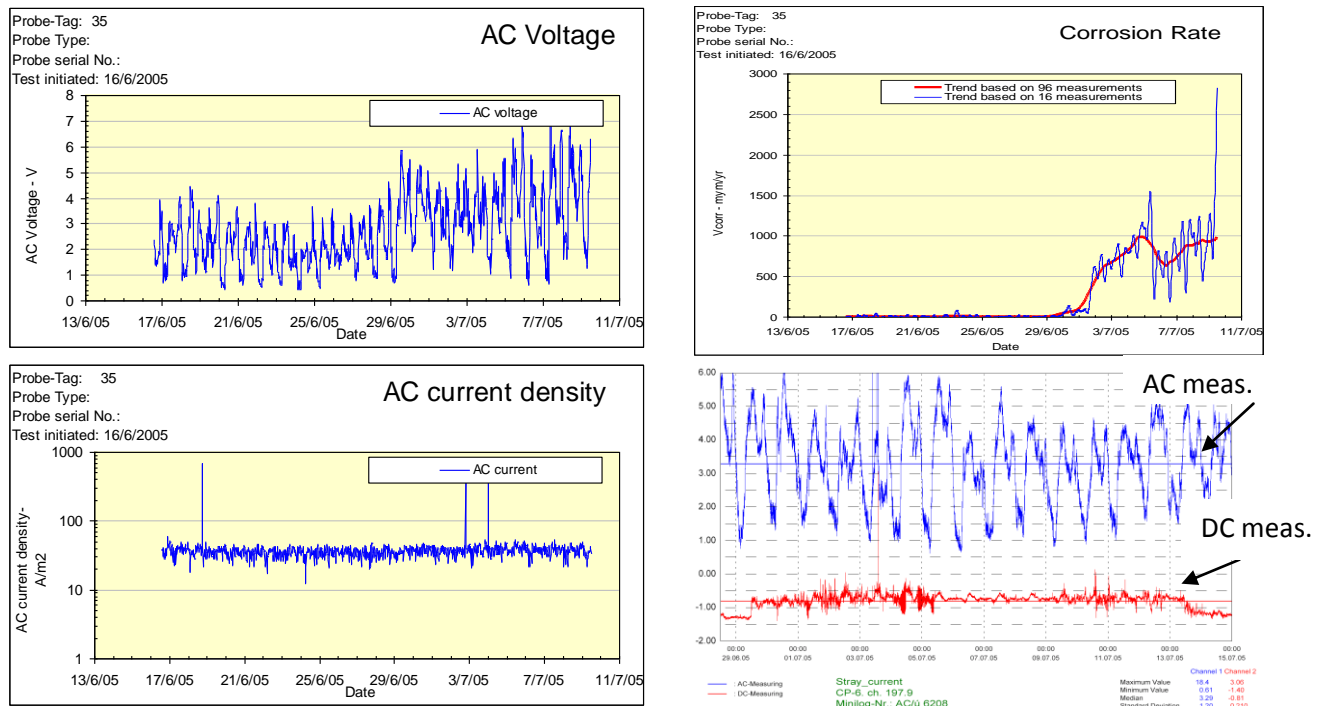


Fig. 9. Corrosion rate, AC voltage, AC current density and DC potential vs. time (case study no.3).

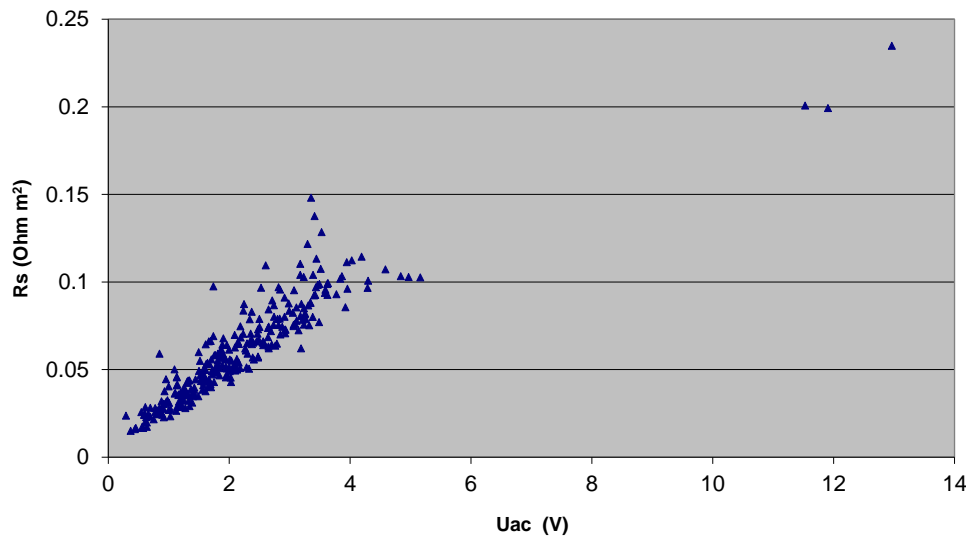


Fig. 10. Fluctuation of spread resistance with AC voltage - case studies no.3 and no.4.

In this case, the AC current density did not play an important role in the corrosion process, since the behavior of the probe was characterized by an increase of spread resistance every time the AC voltage was amplified and vice versa (Fig. 10), i.e. the spread resistance variations followed the variations in AC voltage. This AC effect on the spread resistance was the opposite of that detected in the case study no.1 (Fig.6). It could be attributed to specific soil components giving rise to the formation of resistive

deposits on the metal surface, which enhance the spread resistance at higher AC voltage levels. It resembles a kind of reversible electrodeposition by AC.

Case study no. 4 characterized by corrosion from telluric currents

The case study no.4 referred to a recording on the same ER probe as in Case study no. 3, but about 1 month earlier. It was possible to detect corrosion caused by telluric currents [10], a phenomenon independent of AC corrosion. This is illustrated in Fig.11 showing the correlation of corrosion rate with the Kp index of geomagnetic activity which is a number - ranging from 0 to 9 - indicating intensity of telluric activity. A brief period of increased corrosion rate coincided with a peak in geomagnetic activity. The CP potentials showed a severe disturbance at the same time (Fig. 12). In this case, AC corrosion did not occur. Although a spike (see arrows in Fig.11) of the AC voltage from 2 to 12 V was recorded for a short time (lasting 2-3 hours), it was not accompanied by AC corrosion, while at the same time the AC current density increased only slightly, being always below the threshold of 100 A/m², as a result of the aforementioned increase of spread resistance upon rise in AC voltage. Moreover, it is believed that in areas susceptible to AC corrosion, telluric current corrosion may be hidden by AC corrosion. It may therefore be revealed if AC mitigation takes effect.

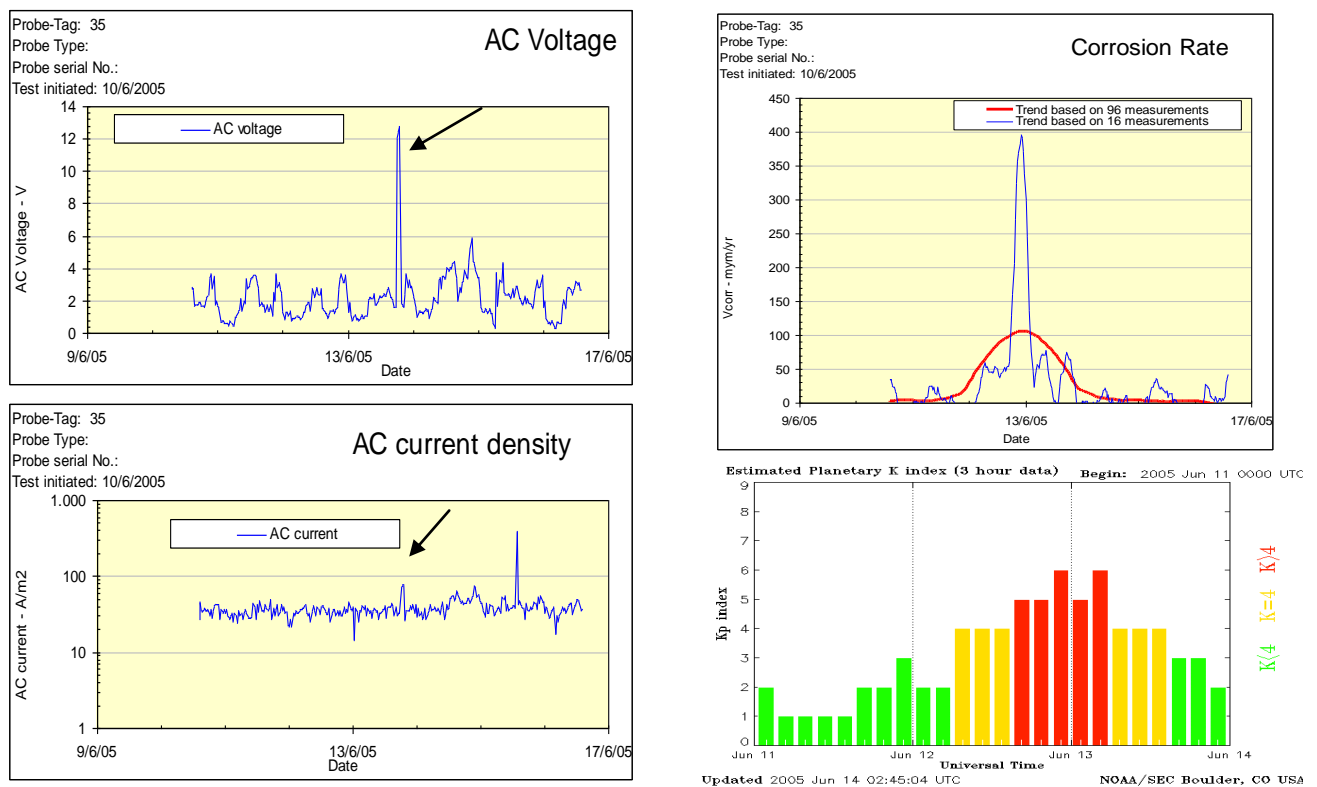


Fig. 11. Corrosion rate, AC voltage, AC current density and telluric activity index Kp vs. time (case study no. 4).

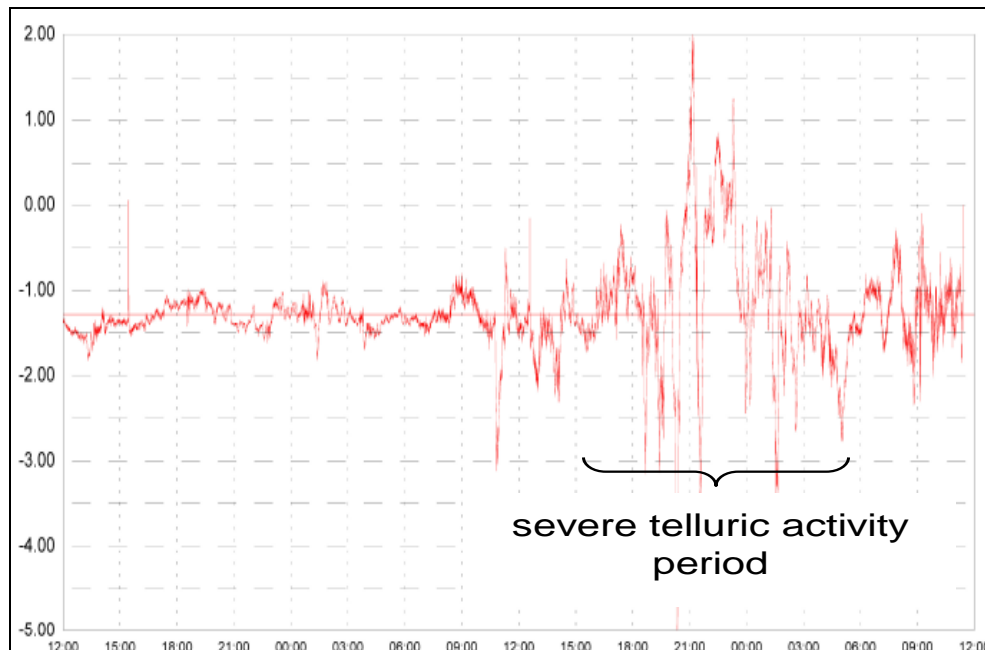


Fig. 12. DC potential recording for case study no. 4.

Comparison of corrosion rate measured by ER probes with the metal loss findings of MFL In-Line Inspection

The accuracy of the MFL method for detection of the size of corrosion defects has been reported to be effective enough only for diameter of metal losses greater than three times the pipe wall thickness [15,16], i.e. where in the present case, for average metal loss diameter over 30mm. Additionally, even in this case, the accuracy of their depth was only $\pm 10\%$ for the wall thickness with a level of confidence only 80%, i.e. for a metal thickness of 10mm, it is $\pm 1\text{mm}$. In several cases, the stated detection limits are in the range from 1 to 2mm with a minimum confidence level $\pm 1\text{mm}$ up to $\pm 2\text{mm}$ [15]. Thus consistent results of MFL ILI inspection are more reliable for larger defects. As the deepest depth of metal loss, detected by the MFL ILI method was about 2,5 mm, the accuracy of the assessment of metal loss size, particularly the depth of metal loss, is close to the error limits. The relevant experience of pipelines in Germany, after a series of inspections and tests [15-17] led to the reported data in Table 2 for the accuracy of the MFL inspection.

Table 2. Accuracy of MFL ILI results for metal losses on pipeline surface

Relative distance of metal loss feature from pipe appurtenances.	High accuracy' Error <0,1m
Orientation of metal loss position on the circumference of pipe	High accuracy' Error ± 15 min
Depth of metal loss	Deviations from -30% up to +100% [15] Deviations from -50% up to +20% [16]
Length / Width of metal loss	Deviations up to $\pm 30\%$

The maximum average corrosion rate obtained from ER probes, at least during the first months of exposure to the corrosive environment, amounted to 2mm/yr. This was a warning, indicating an increased probability of severe corrosion during longer intervals, although this could not be supported by long-term data logging of corrosion rates, as there are currently no such data available.

However, by considering the external metal loss findings from ILI MFL inspection carried out in the pipeline under study in the same CP area, it was found that their maximum depth did not exceed 2,54mm. The inspection was carried out after 8 years of the pipeline operation in 50 bar pressure while buried for almost 10 years. Assuming the metal loss of 2,54mm was due to corrosion, corresponded to a mean maximum corrosion rate scarcely over 0,3mm/yr. This corrosion rate was in line with relevant results from ILI data in different pipeline sections. Thus, the corrosion rates estimated from ILI results were considerably lower than those taken from ER probes findings. These lower corrosion rates were supported by the fact that the natural gas pipeline had not been subject to a gas leak or other disturbing fault relating to pipe integrity. It was thought likely some of the following scenarios to account for it:

- AC corrosion in the long term slows down considerably. This could be a likely scenario, as the corrosion products can increase the incubation time until onset of corrosion. However, it cannot be corroborated since there is no data available.
- The very few pipeline coating defects (due to the highly insulating nature of the coating material as well as the high quality of pipeline installation) are in such environmental conditions that do not cause any significant corrosion. This is considered one of the least likely scenarios due to statistical reasons.
- All defects in the coating of the pipeline are too small (eg $<0,1 \text{ cm}^2$) or too large (e.g. $> 5\text{cm}^2$), so AC corrosion rates in both cases are less rapid since the highest AC corrosion rates occur at coating defects of surface area approaching 1cm^2 [18]. This is considered one of the least likely scenarios for statistical reasons too.
- The inherent shortcomings and the relatively large error of the MFL method (see Table 2) in assessing the dimensions of metal loss increase by reasons such as:
 - The small size of the metal losses caused by AC corrosion.

- The magnetic properties of the AC corrosion products.

Of the main products from AC corrosion is magnetite [19], a material well known for its magnetic properties. The magnetite, which can stick to the metal surface, could be nearly detected as metal, consistently enabling underestimation of the size of AC corrosion defects.

Eventually, in areas suspect of AC corrosion, alternative corrosion and CP inspection techniques should be additionally implemented.

Conclusions

Decisive factors associated with AC corrosion were the AC current density and the spread resistance. The results from ER probes installed at various locations along the pipeline exhibited diverse behaviors associated with variety in electrical interference and local soil conditions. Parameters such as passivation phenomena and variations of spread resistance, the CP level, the magnitude of AC and DC current density played an important role. Areas deserving special attention for AC corrosion risk were those with high soil conductivity.

The corrosion behavior of ER probes was categorized into four case studies.

In case study no. 1, an aggressive form of AC corrosion was developing in relatively low AC voltage (around 1V). It was dramatically accelerated by a cathodic shift towards moderate CP levels (more anodic than -2V). This type of ac corrosion occurred in very conductive soil, leading to minimum spread resistance. The safe AC voltage limit turned out approximately 0,5V, a threshold often being exceeded in spite of the operation of AC mitigation DC decoupling devices. AC corrosion was consistent with the criterion of 100A/m^2 .

A relationship between spread resistance and induced AC voltage was detected, deserving thorough investigation, as it appeared to be related to the mechanism of AC corrosion. It is important that during this type of AC corrosion, the spread resistance was significantly dropping at every AC voltage peak and vice versa, thus AC current density exceeded the safe limit of 100A/m^2 at every slight increase in the AC voltage.

In case study no. 2, a very aggressive AC corrosion occurred at relatively high AC voltage level (in the range 10-30V) in a conductive corrosive soil environment leading to low spread resistance and extremely high AC and DC current densities. There was no obvious relationship between spread resistance and AC voltage.

In case study no. 3, AC corrosion was initiated upon CP interruption/fault.

Case study no. 4 featured a moderate corrosion for a short time of intense geomagnetic activity. This corrosion type was ascribed exclusively to telluric currents, being independent of AC corrosion.

By comparing with case study no.1, in case studies no.3 and no.4, the spread resistance was characterized by the opposite dependence on AC voltage. The higher AC voltage level seemed to promote the depositing of a surface layer which increased the spread resistance; thereby any increase of the AC voltage was insufficient to result in AC current density beyond the safe limit of AC corrosion risk.

Summing up, it became obvious the importance of closer monitoring of the CP system operation and the criticality of CP potential control within certain limits.

The ER probes method turned out a valuable diagnostic tool which helped to clarify the types of AC corrosion. It also enabled identification of pipeline areas prone to AC corrosion while assisting in the assessment of the effectiveness of measures applied to mitigate AC corrosion risk.

Without disregarding the usefulness of MFL ILI technique, in terms of AC corrosion the results of such inspection must be treated with caution, as the weak accuracy of MFL method can be aggravated by the magnetic corrosion products and the fairly small dimensions of AC corrosion defects.

References

1. Gummow, R. A., 1999. Cathodic protection considerations for pipelines with AC mitigation facilities, Report for PRCI and AGA, PR-262-9809.
2. Gummow, R.A., Boteler, D.H., Trichtchenko, L., 2002. Telluric and Ocean Current Effects on Buried Pipelines and their Cathodic Protection Systems. PRCI, PR-262-0030.
3. Boteler, D.H., and Seager, W.H., 1998. Telluric currents: A meeting of theory and observation, *Corrosion NACE*, 54 (9), 751-755.
4. Nielsen L.V. and Nielsen K.V., 2003. Differential ER-technology for measuring degree of accumulated corrosion as well as instant corrosion rate, *In: NACE Corrosion 2003* paper No. 03443.
5. Nielsen L.V., Nielsen K.V., Baumgarten B., Breuning-Madsen H., Cohn P., Rosenberg H., 2004. AC-induced corrosion in pipelines: Detection, characterisation and mitigation, *NACE Corrosion 2004* paper No. 04211.
6. Nielsen L.V. and Galsgaard F., 2005. Sensor technology for on-line monitoring of AC-induced corrosion along pipelines, *In: NACE Corrosion 2005*, paper No. 05375
7. Kioupis, N., Kouloumbi, N., Batis, G., Asteridis, P., 2003. Study of the effect of AC-interference and AC-mitigation on the cathodic protection of a gas pipeline, *In: CeoCor 6th International Conference, Giardini-Naxos Sicily 13-16 May 2003*. Brussels : CeoCor proceedings Sector A paper 13.
8. Kouloumbi N., Batis G., Kioupis N., Asteridis P., 2002. Study of the effect of AC-interference on the cathodic protection of a gas pipeline, *Anti-Corrosion Methods and Materials (ACMM)*, 49 (5), 335-345.
9. CEN/TS 15280:2006. *Technical Specification, Evaluation of a.c. corrosion likelihood of buried pipelines–Application to cathodically protected pipelines*, Brussels 2006.
10. Kioupis, N. and Maroulis K., 2006. AC-Corrosion Detection On Electrical Resistance Probes Connected To A Natural Gas Transmission Pipeline, *In: 8th International Conference Pipeline Rehabilitation & Maintenance*, Instabul, Turkey, 11-15 Sept. 2006.
11. Kioupis, N., PhD thesis, *Induced AC interference effects on cathodic protection of buried in soil metallic pipelines*, National Technical University of Athens, May 2009.

12. Büchler, M. and Schöneich, H.-G., 2009. Investigation of alternating current corrosion of cathodically protected pipelines: Development of a detection method, mitigation measures and a model for the mechanism . Corrosion NACE, 65 (9), 578-586.
13. I. Ibrahim, H. Takenouti, B. Tribollet, X. Campaignolle, S. Fontaine, P. France, H.-G. Schoeneich, Harmonic Analysis Study of the AC Corrosion of Buried Pipelines Under Cathodic Protection CORROSION 2007, March 11 - 15, 2007, Nashville, Tennessee, paper no. 07042.
14. Bosch, R.W. and Bogaerts, W.F., 1998. A theoretical study of ac-induced corrosion considering diffusion phenomena, *Corrosion Science*, 40 (2/3), 323-336.
15. Ahlers, M. and Schöneich, H.-G., 2000. Smart pigging – a contribution to the monitoring of the anti-corrosion protection systems on pig-inspectable high-pressure gas transmission pipelines, *3R International*, 39 (7), 400-406.
16. Ahlers, M., 2000. Ermittlung von Korrosionsschäden an erdverlegten Rohrleitungen durch intelligente Molchung und Intensivmessung-Möglichkeiten und Grenzen. In: *CeoCor 5th International Conference, 9- 12 May 2000 Brussels*. CeoCor proceedings Sector A paper 15.
17. Ahlers, M., Geiser, J., Schöneich, H.-G., 1998. Investigation of coating quality on new laid pipelines. *3R International*, 37 (6), 341-345.
18. Heim, G. and Peez, G. 1992. The Influence of alternating currents on buried and cathodically protected high pressure gas pipelines, *gwf Gas-Erdgas* 133 (3), 137-142.
19. CeoCor 2001. *A.C. corrosion of cathodically protected pipelines – Guidelines for risk assessment and mitigation measures*. Brussels : APCE 2001.